



Columnar metallomesogens derived from unsymmetrical pyrazoles

Shih-Yu Chou^a, Chun-Jung Chen^a, Shao-Ling Tsai^a, Hwo-Shuenn Sheu^b,
Gene-Hsiang Lee^c, Chung K. Lai^{a,*}

^a Department of Chemistry, National Central University, Chung-Li 32054, Taiwan, ROC

^b National Synchrotron Radiation Research Center, Hsinchu 30077, Taiwan, ROC

^c Instrumentation Center, National Taiwan University, Taipei 10660, Taiwan, ROC

ARTICLE INFO

Article history:

Received 25 September 2008

Received in revised form 18 November 2008

Accepted 26 November 2008

Available online 30 November 2008

ABSTRACT

The synthesis and mesomorphism for two series of unsymmetrical pyrazoles and their nickel(II) complexes were described. This is the first example of nickel complexes exhibiting columnar phase. The derivatives with two alkoxy chains exhibited smectic A or smectic C phases; however, all derivatives with four alkoxy chains formed hexagonal columnar phases. In contrast, all nickel(II) complexes **1a** formed hexagonal columnar phases. The crystal and molecular structures of 1-(4-propyloxyphenyl)-2-(3-(4-propyloxyphenyl)-1H-pyrazol-5-yl)ethanone were determined, and it crystallizes in the triclinic space group *P*-1. The overall molecular shape is considered as rod-shaped. The pyrazole and one phenyl ring were coplanar, however, they were not coplanar with other phenyl ring by a dihedral angle of ca. 66.2°. A dimeric structure formed by an *intermolecular* H-bond (2.11 Å) and a weak π - π interaction (3.51 Å) was observed, which was probably attributed to the formation of the mesophase. The XRD experiments confirmed their structures of the mesophases.

© 2008 Elsevier Ltd. All rights reserved.

1. Introduction

The interest in metallomesogens¹ or metal-containing liquid crystals (MCLCs) has been extensively expanded during past years. Modern synthetic knowledge allows researchers to access tailor-made materials with predictable properties, particularly in the field of liquid crystalline materials. More and more examples^{1,2} with particular structures and/or novel physical properties were obtained by incorporation of a metal ion or metal ions into an organic fragment. The coordination geometry of the central ion is often important in determining the mesogenic materials since it often alters the overall molecular shape. Metal ions, for example, d⁹-Cu²⁺, d⁸-Ni²⁺, or d¹-VO²⁺ with square-planar coordination (SP) were used the most; however, metal ions with tetrahedral (*T_d*) or octahedral² (*O_h*) coordination were relatively lesser. In addition, use of paramagnetic (Cu²⁺, Mn²⁺, and VO²⁺) or diamagnetic ions (Cu¹⁺, Pd¹⁺, and Rh¹⁺) might alter the magnetic behavior of the metallomesogenic materials. Metallomesogens obtained often have properties quite distinct from their precursors, such as mesomorphism, color, magnetic behavior, and other physical properties. Metallomesogens might be generated from non-mesogenic precursors, and vice versa. Pyrazoles,³ cataloged as heterocyclic ligands, have been widely applied in inorganic, organometallic, and

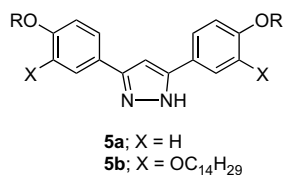
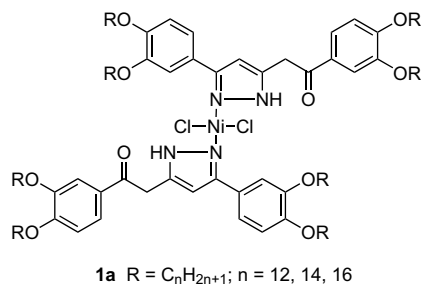
bioinorganic chemistry.^{3,4} They are electron-deficient or electron acceptors, therefore, a local dipole of donor-to-acceptor (D-A) interaction was easily induced within molecules or between molecules. Interest in such systems stems from their diverse structures and known chemistry. Two nitrogen atoms on the pyrazole ring are often capable of binding to metal ions (i.e., M¹⁺ and M²⁺). Two bonding modes are feasible. One N atom can donate an electron lone pair to metal ions, leaving the pyrazolic -NH as a free group, and this type of bonding is particularly efficient with M²⁺ ions. On the other hand, the other N atom can be deprotonated (pyrazolate anion) with a base, binding to M¹⁺ ions. This type of pyrazole anion, important as a bichelating ligand, was often applied to generate complexes with an *exo*-bidentate structure.^{4a,5} Most of structures with divalent metal ions formed were of ML₂ and metal ions used were dominantly first-row transition-metal ions. However, trinuclear pyrazolate complexes formed by monovalent coinage metal,⁶ such as Cu¹⁺, Ag¹⁺, and Au¹⁺, were also prepared. Some of neutral metal complexes⁷ having fluorinated ligands are of particular interest as emitting materials for molecular light-emitting devices (MOLEDs). Fluorination facilitated thin-film fabrication process and also the presence of a closed-shell transition metal should enhance the phosphorescence efficiency. Some copper(I) complexes with trinuclear⁸ [Cu(dmpz)]₃ or tetranuclear⁹ structures [Cu(dppz)]₄ were found to be useful catalysts on organic reactions.

By contrast, known examples of mesogenic pyrazoles and derived metallomesogens¹⁰ were relatively rare. Most reported structures were mononuclear, whereas, a few examples of dinuclear

* Corresponding author. Tel.: +886 3 4259207; fax: +886 3 4277972.
E-mail address: cklai@cc.ncu.edu.tw (C.K. Lai).

and trinuclear complexes were also known. More examples were prepared and studied since the first example containing 3,5-disubstituted phenylpyrazole¹¹ exhibiting SmA and SmC phases was reported in 1992. Among them, rhodium(I) and palladium(II) are used the most to generate the metallomesogens. These two metal ions were all d^8 electronic configurations and square-planar preferred in coordination geometry. A nonmesogenic ZnL_2Cl_2 ($L=3,5$ -bis(*p*-decyloxyphenyl)pyrazole)¹² was reported, and the mesophase was improved by a structural modification of ligand.¹³ Crystallographic data on other similar pyrazole related zinc complexes¹⁴ showed that zinc centers were all tetrahedral. Metal center with a tetrahedral geometry resulted in an unfavorable angle between central cores, precluding the formation of mesomorphism. The zinc complex also exhibited fluorescence properties.¹³ A few square-planar Rh^{1+} complexes, such as $[RhCl(CO)_2(Hpz^R)]$,^{15a} $[Rh(\mu-pz^R)(CO)_2]_2$,^{15b} $[Rh(\mu-pz^{PP})(COD)]_2$,^{16a} and $[Rh(\mu-pz^{BP})(COD)]_2$,^{16a} and $[Rh(Cl)(NBD)(Hpz^R)]$ ^{16b} containing substituted pyrazoles with long-chained substituents were found to be mesogenic. Palladium(II) fragments, $PdCl_2$ ^{17a-c} and $Pd(\eta^3-C_3H_5)^+$ ^{17d,e} were also used to generate metallomesogens, $[PdCl_2(pz^Rpy)]$ and $[Pd(\eta^3-C_3H_5)(Hpz^R)]^+BF_4^-$. Example of bimetallomesogens, $[Pd(\eta^3-C_3H_5)(\mu-pz^R)]_2$ ¹⁸ containing bridged 3,5-disubstituted pyrazolate ligands was reported. Most of mesogenic pyrazoles and their related metallomesogens exhibited smectic phases. However, a few examples of pyrazole-derived metallomesogens formed by mononuclear- Cu^{1+} , Rh^{1+} , and trinuclear- Au^{1+} complexes¹⁹ exhibiting columnar phases were also prepared and studied.

In this work, we describe herein the preparation and mesomorphic studies of two new series of heterocyclic pyrazoles **2a,2b** and their nickel complexes **1a**. These compounds showed a strong chain density dependence on the formation of the mesomorphic properties. All derivatives **2b** with two alkoxy chains exhibited smectic A or smectic C phase, however, other series of derivatives **2a** with four alkoxy chains formed hexagonal columnar phases (Col_h). In contrast, all nickel(II) complexes **1a** displayed hexagonal columnar phases. Similar compounds, 3,5-di(4-*n*-alkoxyphenyl)pyrazoles **5a** have been previously prepared and also their mesomorphic properties studied. They all exhibited enantiotropic smectic A, C or/and X phases over a wide range of temperatures. Crystallographic data indicated that the H-bonding was probably attributed to the formation in such systems. On the other hand, a series of compounds **4** with a similar structure was also prepared in order to understand the effect of H-bonding in this type of pyrazole ligands. A dimeric structure, supported by crystallographic data formed by an *intermolecular* H-bonding was also observed, which might facilitate the formation of the mesophases. This is the first example of nickel complexes derived from pyrazoles exhibiting hexagonal columnar (Col_h) phases.



2. Results and discussions

2.1. Synthesis

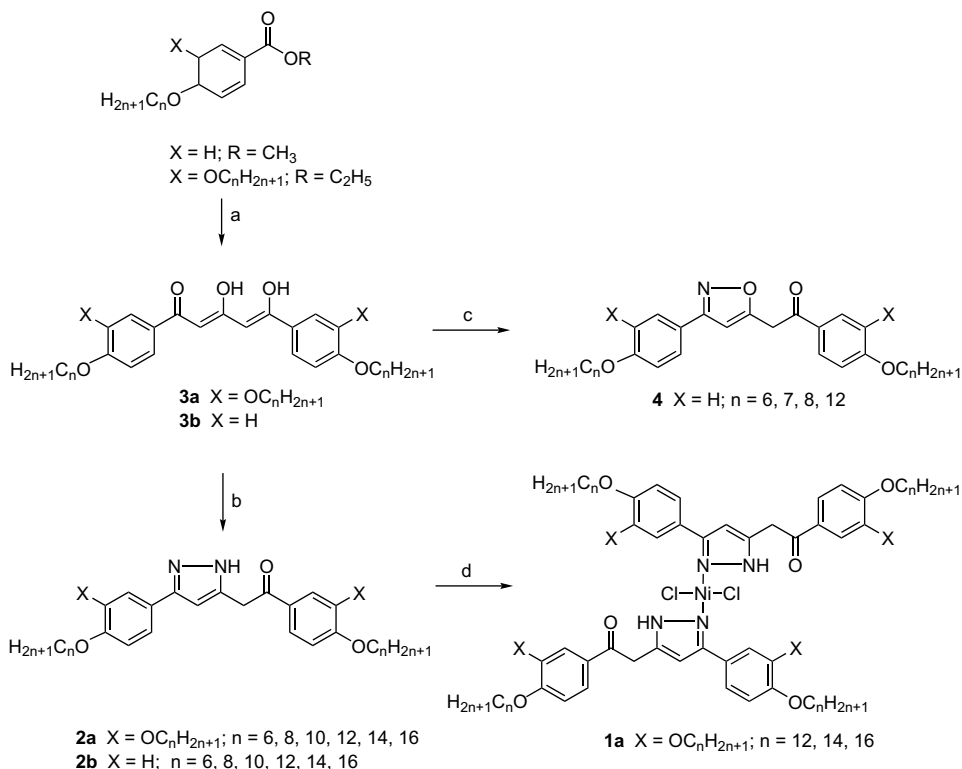
The synthetic pathways followed to prepare compounds **1–4** are summarized in Scheme 1. All precursors **3** were prepared according to the literature procedures^{19a,20} using cross-Claisen condensation reactions. The further condensation reactions of 1,3,5-triketones and hydrazine monohydrate in refluxing absolute ethanol produced the pyrazole derivatives **2** as off-white solids with a yield of ca. 65–84%. All compounds were characterized by 1H , ^{13}C NMR spectroscopy, mass spectroscopy, and elemental analysis. The solubility in $CDCl_3$ for some of pyrazole derivatives was poor, so their ^{13}C NMR spectra were not possibly obtained. Three tautomers for pyrazoles **2** are structurally possible. On the 1H NMR spectra, only two characteristic peaks at δ 6.37–6.61 and δ 4.29–4.57, assigned to pyrazole-H ($-CHC=N$) and keto-H ($-CH_2CO$) were observed, however, the pyrazole-H ($-NH$) often occurred at ca. δ 11.60–12.60 was not observed. In contrast, two other characteristic peaks at δ 5.80 and δ 6.20 assigned to olefinic methane-H ($-CH=C$) of 1,3,5-triketones **3** were also disappeared. On the other hand, the observation of one peak at ca. δ 193.6 on ^{13}C NMR spectra assigned to keto $-CH_2C=O$ confirmed the isomer **2** as the most stable structure among three isomers. Also a persistent solution in $CDCl_3$ did not show an apparent change on 1H NMR spectrum. The further reactions of pyrazole **2a** with $NiCl_2$ in refluxing C_2H_5OH/THF produced the nickel complexes **1a**. The structure of nickel complexes was tentatively proposed as drawn due to a lack of single crystallographic analysis. Nickel atom was coordinated as square-planar geometry to two nitrogen atoms with lone electron pairs, leaving the other two nitrogen atoms as free amine-HH. The similar reactions with $CuCl_2$ to prepare copper complexes were not successful for an unknown reason.

2.2. The X-ray single crystallographic data

A single crystals of the non-mesogenic pyrazole **2b** ($n=3$) suitable for crystallographic analysis were obtained by slow vaporization from CH_3Cl at room temperature and their structures resolved. Figure 1 shows the molecular structure with the atomic numbering schemes. Table 1 lists their crystallographic and structural refinement data for the molecule. The overall molecular shape of crystal was considered as a linear structure with a length of ca. 21.15 Å. The central pyrazole ring and phenyl rings were coplanar; however, they were not coplanar to the other phenyl ring. A dihedral angle of 66.2° was measured. Unsurprisingly, an *intermolecular* H-bond between O4 and H2 atoms was observed, and the distance was measured by ca. 2.11 Å. The distance between N1 and N2 atoms (see Table 2) was 1.356 Å, similar to other known pyrazole. The bond length of 1.218 Å (C5–O1 atom) and its bond angle of 121.3° ($\angle C1-C5-C4$) supported the structure **2** (not **2'** or **2''**) as the most stable tautomers. The carbonyl group was existent with a free C=O moiety. In the unit cell, molecules were packed with a head-to-head arrangement. Such dimeric structure facilitated a better packing both in the solid or/and the liquid crystal state. However, *intermolecular* H-bonding was not observed. On other hand, a $\pi-\pi$ interaction of 3.51 Å was also observed, as shown in Figure 2.

2.3. Mesomorphic properties

The mesomorphic behavior of compounds **1–4** was studied by differential scanning calorimetry (DSC), polarizing optical microscopy (POM), and powder X-ray diffractometry (XRD). The phase transitions and thermodynamic data for compounds **1–4** are



Scheme 1. Reactions and conditions: (a) Acetone (0.5 equiv), NaH (6.0 equiv), refluxing in dimethoxyethane, 48 h, 72–89%; (b) $N_2H_4 \cdot H_2O$ (10.0 equiv), refluxing in ethanol, 12 h, 65–84%. (c) $NH_2OH \cdot HCl$ (1.1 equiv), refluxing in ethanol, 12 h, 70–76%; (d) $NiCl_2$ (0.55 equiv), refluxing in ethanol/THF, 24 h, 92–95%.

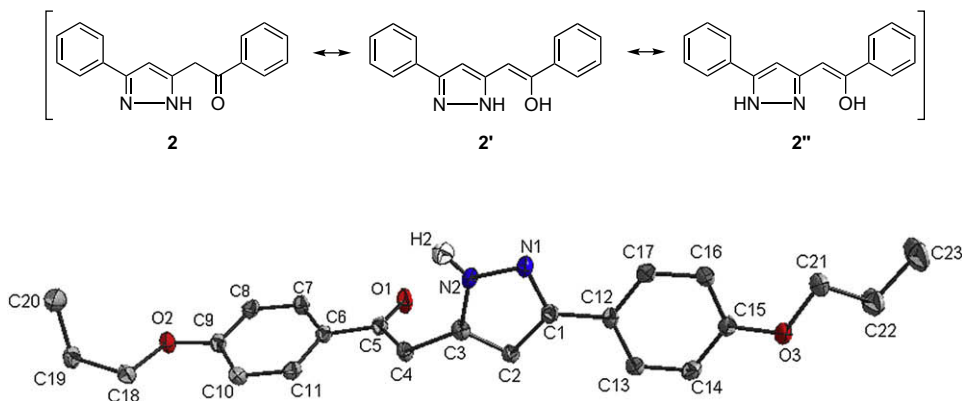


Figure 1. An ORTEP plot for compound **2b** ($n=3$) with the numbering scheme, and the thermal ellipsoids of the non-hydrogen atoms are drawn at the 50% probability level.

summarized in Tables 3 and 4. The mesomorphic results indicated that the formation of mesophases in pyrazolate compounds **2** was strongly dependent of alkoxy chain density. All compounds **2b** with two alkoxy chains displayed enantiotropic smectic A or smectic C phase; however, all compounds **2a** with four alkoxy chains formed enantiotropic columnar phases. Among compounds **2b** only derivative with shorter chains ($n=6$) exhibited SmA phase and all other compounds with longer chains ($n=8, 10, 12, 14, 16$) formed SmC phase. A slight decrease both in the melting temperatures and clearing temperatures accompanying an increase in the alkoxy chain length was observed. However, the temperature range of SmA or SmC phase was between $13.7^\circ C$ ($n=6$) and $33.3^\circ C$ ($n=10$) on heating process. The pyrazolate derivative $n=10$ has the widest temperature range of SmC phase. Under the optical microscope, a typical fan-shaped texture with homeotropic domain for SmA or without homeotropic area for SmC phases, respectively, was

observed upon slow cooling from their isotropics, as shown in Figure 3. A series of pyrazoles **5a** with similar structures was previously prepared and studied. These compounds exhibited N, SmA, SmC, or/and SmX phases depending the carbon chain lengths. However, all compounds **2b**, particularly with the lower carbon chain length have both lower clearing temperatures, i.e., $198^\circ C$ (**5a**, $n=6$) $> 165^\circ C$ (**2b**, $n=6$) and narrower temperature range, i.e., $39.5^\circ C$ (**5a**, $n=6$) $> 11.3^\circ C$ (**2b**, $n=6$) of mesophases than those of compound **5a**. This lowering in clearing temperatures might be attributed to the ketonate group ($-CH_2C=O$) group next to the pyrazolate ring in **2b**. The ketonate $-CH_2C=O$ group was found not coplanar to the pyrazolate ring (i.e., see discussion in single crystal data), which tended to reduce the intermolecular interaction both in crystal and mesogenic states.

The mesomorphic behavior was distinctive when the total alkoxy chains' numbers increased to four in compound **2a**. Under the

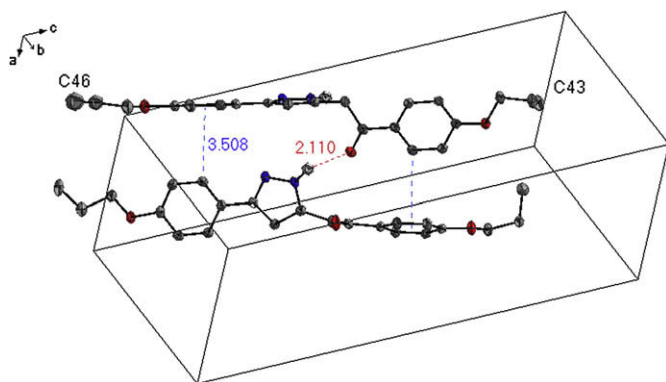
Table 1
Crystal and refinement data for compound **2b** ($n=3$)

Compound	2b ($n=3$)
Empirical formula	C ₂₃ H ₂₆ N ₂ O ₃
Formula weight	378.46
T/K	150(2)
Crystal system	Triclinic
Space group	$P\bar{1}$
$a/\text{Å}$	7.6828(5)
$b/\text{Å}$	11.4540(7)
$c/\text{Å}$	22.2399(14)
$\alpha/^\circ$	90.630(2)
$\beta/^\circ$	97.405(2)
$\gamma/^\circ$	94.267(2)
$U/\text{Å}^3$	1935.0(2)
Z	4
$F(000)$	808
$D_c/\text{Mg m}^{-3}$	1.299
Crystal size/mm ³	0.40×0.32×0.05
Range for data collection/ $^\circ$	0.92–27.50
Reflections collected	25,735
Data, restraints, parameters	8854/0/507
Independent reflections	8854 [$R_{\text{int}}=0.0508$]
Final $R1$, $wR2$	0.0728, 0.1614

Table 2
Selected bond distances [Å] and angle [°] for compound **2b** ($n=3$)

Bond distances			
N(1)–N(2)	1.356(3)	N(2)–C(3)	1.348(3)
N(1)–C(1)	1.331(3)	C(1)–C(2)	1.407(3)
C(2)–C(3)	1.364(3)	O(1)–C(5)	1.218(3)
C(1)–C(12)	1.469(3)	C(3)–C(4)	1.499(3)
C(4)–C(5)	1.515(3)		
Bond angles			
C(1)–N(1)–N(2)	104.15(18)	C(3)–N(2)–N(1)	112.92(18)
N(1)–C(1)–C(2)	111.10(19)	N(1)–C(1)–C(12)	120.30(19)
C(3)–C(2)–C(1)	105.6(2)	N(2)–C(3)–C(2)	106.21(19)
N(2)–C(3)–C(4)	122.2(2)	C(2)–C(3)–C(4)	131.6(2)
C(3)–C(4)–C(5)	114.49(18)	O(1)–C(5)–C(6)	120.9(2)
O(1)–C(5)–C(4)	121.3(2)	C(6)–C(5)–C(4)	117.81(19)

Symmetry transformations used to generate equivalent atoms.

**Figure 2.** A side view of the molecular packings in the unit cell was shown. The molecular length (C46–C'43=ca. 21.25 Å), intermolecular H-bonding (ca. 2.110 Å), and a π - π interaction (ca. 3.51 Å) were shown.

optical polarized microscope, they melted into viscous phases upon slow heating, and a typical pseudo-focal conics or fan-shaped texture (shown in Fig. 4) with homeotropic behavior was observed on cooling from their isotropic states. This type of texture was characteristic of hexagonal columnar (Col_h) phases. On the DSC analysis, these compounds all exhibited two enantiotropic transitions, crystal-to-columnar ($\text{Cr} \rightarrow \text{Col}_h$) and columnar-to-isotropic ($\text{Col}_h \rightarrow \text{I}$). The clearing temperature slightly increased with side

Table 3
The phase transitions^a and temperatures of compounds **2a, 2b**

Compound						
2b ; $n=6$	8	Cr	151.3 (32.2)	SmA	165.0 (9.69)	
			118.8 (29.2)		160.1 (10.4)	
	10	Cr	142.7 (42.0)	SmC	167.6 (11.9)	
			112.7 (39.0)		163.4 (11.5)	
	12	Cr	131.7 (60.4)	SmC	165.1 (13.2)	
			109.0 (60.4)		160.7 (12.1)	
	14	Cr	132.2 (60.7)	SmC	163.0 (11.3)	
			109.5 (55.6)		157.8 (10.9)	
	16	Cr	134.9 (57.8)	SmC	159.0 (9.34)	
			111.5 (57.3)		151.0 (7.74)	
	2a ; $n=6$	8	Cr	68.1 ^b	Col_h	68.8 (2.65)
				45.5 ^b		64.2 (2.63)
10		Cr	63.3 ^b	Col_h	79.9 (2.91)	
			52.3 ^b		74.8 (2.81)	
12		Cr	65.2 ^b	Col_h	91.3 (3.04)	
			54.1 ^b		86.1 (2.95)	
14		Cr	62.5 ^b	Col_h	92.3 (3.13)	
			43.9 ^b		89.0 (3.12)	
16		Cr	45.2 (11.2)	Col_h	89.4 (3.31)	
			28.5 (28.3)		86.1 (3.16)	
16		Cr	62.7 (44.3)	Col_h	82.4 (6.30)	
			47.4 (67.4)		79.7 (1.80)	

^a n =The carbon numbers of alkoxy chains, Cr=crystal, SmA=smectic A, SmC=smectic C, Col_h =hexagonal columnar phase, I=isotropics.

^b Obtained by optical microscope.

Table 4
The phase transitions^a and temperatures of compounds **1a** and **4**

Compound						
4 ; $n=6$	7	Cr	103.8 (40.0)	SmC	108.0 (1.30)	
			60.2 (18.9)		116.2 (4.20)	
	8	Cr	85.1 (22.7)	SmC	118.9 (9.93)	
			53.8 (18.5)		114.5 (9.02)	
	12	Cr	82.2 (23.4)	SmC	124.2 (12.2)	
			52.8 (19.3)		119.5 (11.7)	
	16	Cr	79.1 (23.3)	SmC	133.9 (14.6)	
			69.6 (32.0)		129.3 (14.2)	
	1a ; $n=12$	14	Cr	108.3 ^b	Col_h	117.1 (8.37)
				78.0 ^b		113.9 (7.37)
		16	Cr	115.2 ^b	Col_h	132.8 (4.54)
				89.1 ^b		129.1 (4.31)
16		Cr	110.3 ^b	Col_h	128.4 (5.85)	
			87.6 ^b		125.3 (5.10)	

^a n =The carbon numbers of alkoxy chains, Cr=crystal, SmA=smectic A, SmC=smectic C, Col_h =hexagonal columnar phase, I=isotropics.

^b Obtained by optical microscope.

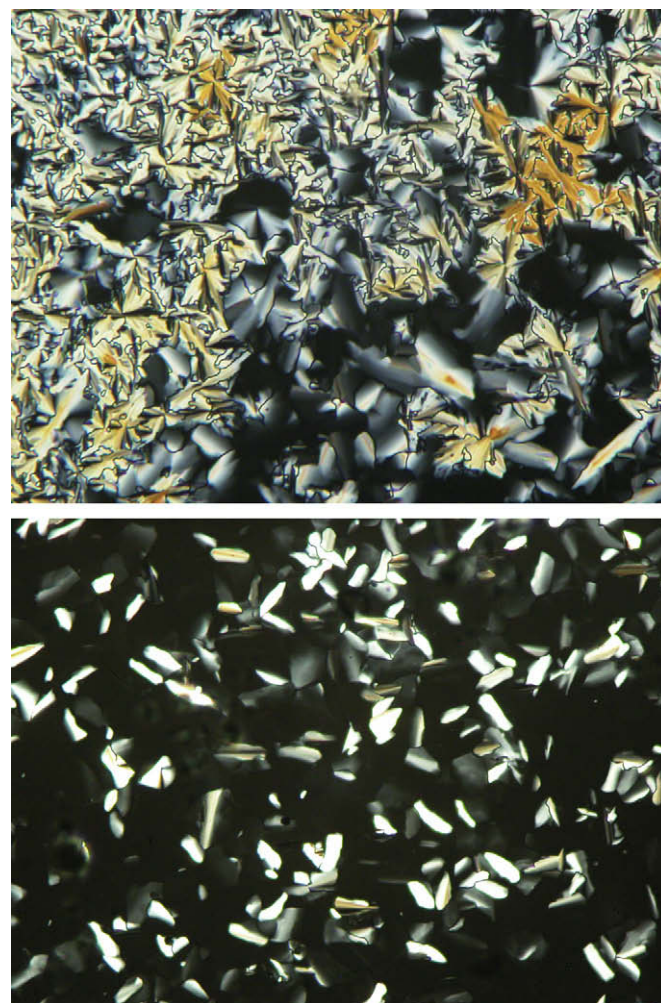
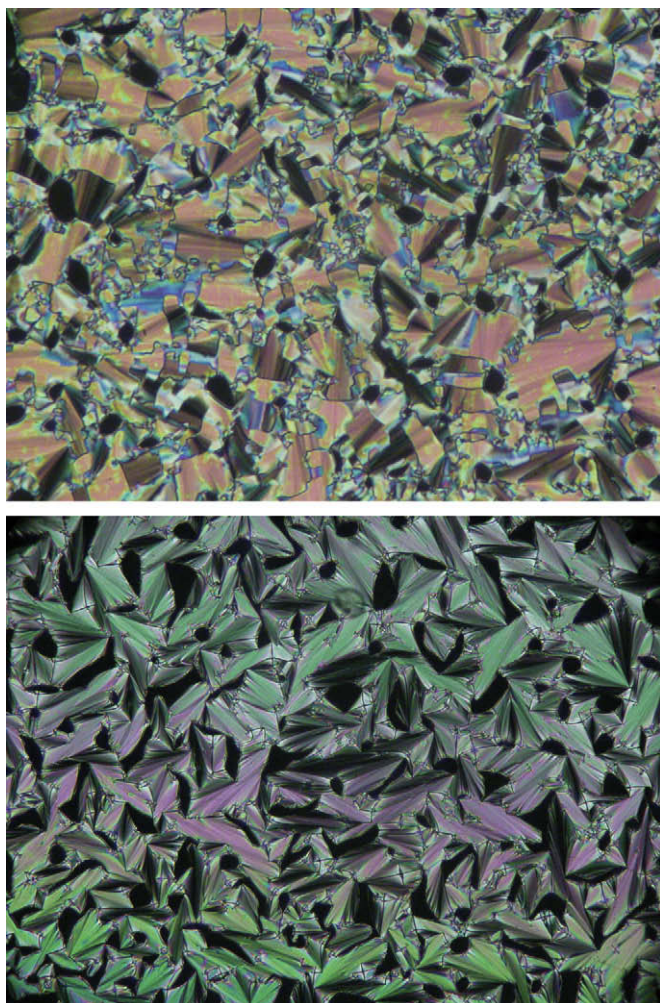


Figure 3. Optical textures observed by compounds **2b**. Top plate: SmC phase ($n=12$) at 150 °C and bottom plate: SmA phase ($n=6$) at 155 °C.

Figure 4. Optical textures observed by compounds **2a**. Top plate: Col_h phase ($n=12$) at 86.0 °C, and bottom plate: Col_h phase ($n=6$) at 65.0 °C.

chain length of derivatives $n=6, 8, 10, 12$ and then decreased with derivatives $n=14, 16$. The temperature range of the columnar phases also increased with carbon number, i.e., $\Delta T=0.7$ °C ($n=6$) < 16.6 °C ($n=8$) < 26.1 °C ($n=10$) < 29.8 °C ($n=12$) < 44.2 °C ($n=14$), and reached to $\Delta T_{\max}=44.2$ °C for derivative $n=14$. Interestingly, the overall molecular shape of compounds **2a** was not rod or a disc-shaped. On the other hand, the overall molecular shape of a monomeric molecule was in fact considered as half-disc-shaped. Most of columnar phases reported were formed by molecules with six or eight side chains. A complementary structure was proposed to be made by two correlated monomeric molecules. Two combined half-disc-shaped molecules gave a total number of eight alkoxy side chains, which were then enough to form a columnar phase. The formation of columnar phases in compounds **2a** was probably attributed to the dimeric structure formed via intermolecular H-bonding. The dimeric structure formed by H-bonding was observed in other pyrazolate system.

In order to understand the effect of possible H-bonding on the formation of mesophase in such calamite pyrazolate derivatives, a series of heterocyclic isoxazoles **4** was also prepared and mesomorphic properties compared. All compounds **4** are structurally similar to compounds **2**; however, H-bonding is not possibly induced in compounds **4**. Thermal data indicated that compounds **4** were all mesogenic. The derivative with shorter alkoxy chains ($n=6$) formed SmA at higher temperature and SmC phase at lower temperature, and all other derivatives with longer side chains ($n=7, 8,$

12) exhibited SmC phase only (Fig. 5). The overall molecular shapes of compounds **4** are considered as rod-shaped, slightly bent structures with a bending angle equal to 154–165°, similar to those of pyrazoles. The melting temperature decreased with carbon chain length, i.e., $T_m=103.8$ °C ($n=6$) > $T_m=79.1$ °C ($n=12$), however, the clearing temperature increased with carbon chain length, i.e., $T_{cl}=116.2$ °C ($n=6$) < $T_{cle}=133.9$ °C ($n=12$). The clearing temperature was slightly lower by ca. 29.1 °C ($n=12$) to 48.8 °C ($n=6$) than those of compound **2b**, which might be attributed to the absence of H-bonding. On the other hand, the temperature range of mesophase in compounds **4** was slightly wider than those in compounds **2b**.

Upon coordinated to Ni²⁺ ion, a more discotic molecule resulting from nickel complexes **1a** ($n=12, 14, 16$) were formed. The formation of columnar phases was often found to depend crucially on the side chain density. On the other hand, the side chain density required for the columnar phases was strongly dependent on the size or the flexibility of the core center, i.e., the larger size or the more rigid is the core group, and more side chain density is often needed. The overall molecular shape of compounds **1a** is considered as discotic or round, and eight alkoxy chains appended were enough to form a stable columnar phase. Thermal data were shown in Table 2. All derivatives formed enantiotropic hexagonal columnar phases (Col_h), and two typical transitions of crystal-to-columnar and columnar-to-isotropic were observed on DSC analysis. The melting temperatures were only observed by optical microscope. On the other hand, all clearing temperatures were highly

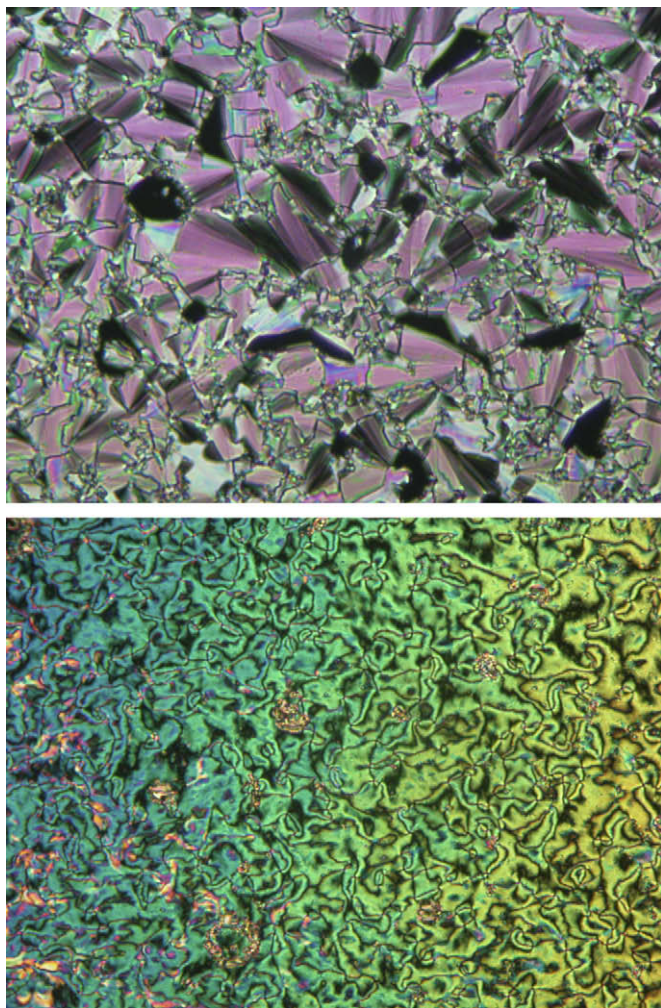


Figure 5. Optical textures observed by compounds **4**. Top plate: SmC phase ($n=12$) at 100.0 °C and bottom plate: SmC phase ($n=6$) at 100.0 °C.

higher than those their ligand derivatives **2a** by 24.0 °C ($n=12$) to 46.0 °C ($n=16$) due to a larger and more rigid core. The temperature range of columnar phases was slightly narrower than those of their homologues **2a**. The Col_h phase was also characterized by optical polarized microscope. A typically pseudo-focal-conic texture (see Fig. 6) with linear birefringent defects on slowly cooling from the isotropic liquid was clearly observed. This observed texture also accompanied by a large area of homeotropic domain is often characteristic for hexagonal columnar phases. In contrast to compound **2a**, the columns in hexagonal phases in compounds **1a** were formed by stacking single molecule (monomeric structure, shown in Fig. 7). The powder XRD results confirmed the structure of the mesophase as Col_h phase. For example, compounds **2a** ($n=12$) and **1a** ($n=12$) both have a similar lattice constant in magnitude of 34.32 Å and 33.82 Å, respectively. The lattice constants were quite consistent with proposed model of a monomeric and dimeric structure formed in compounds **1a** and **2a**, respectively.

2.4. Variable temperature XRD diffraction

Variable-temperature powder XRD diffraction was conducted to confirm the structure of the mesophases. A summary of the diffraction peaks and lattice constants for compounds **1**, **2**, and **4** is listed in Table 5. For compound **2b** ($n=6, 10, 12$), only one strong diffraction peak at lower angle was observed, which corresponded to a layer structure of SmA or SmC phase. The relative intensity of the

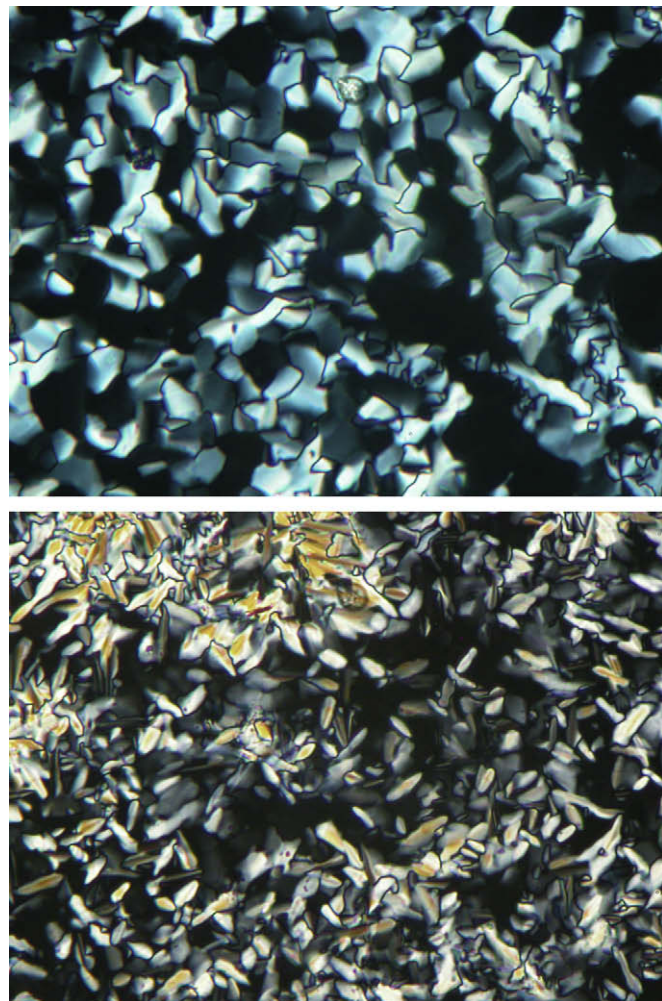


Figure 6. Optical textures observed by compounds **1a**. Top plate: Col_h phase ($n=14$) at 125.0 °C and bottom plate: Col_h phase ($n=12$) at 110.0 °C.

diffraction peak was stronger for SmC phase than that for SmA phase. For example, the derivative $n=6$ gave a diffraction at d 28.7 Å at 130 °C, in contrast, two other derivatives $n=10$ and $n=12$ displayed a strong reflection of d 33.04 Å at 145 °C and d 37.21 Å at 150 °C, respectively. These observed d -spacings were all shorter than those of molecular lengths calculated by MM2 model, which indicated the alkoxy chains of the molecules were probably interdigitated in the mesophase. Compound **4** ($n=6$) also gave a diffraction peak of d 24.47 Å at 109 °C and d 24.08 Å at 96 °C. These types of diffraction pattern corresponded to Miller indices 001 in layer structures of SmA and SmC phases, shown in Figure 8. However, other diffraction peaks of higher orders indexed as 002, 003, and others were not observed. On the other hand, the compounds **2a** ($n=12, 14$) and **1a** ($n=12, 14, 16$) exhibited different diffraction patterns. All these compounds displayed the diffraction pattern of a two-dimensional hexagonal lattice, with one stronger peak and two weaker peaks. These are characteristic of columnar phases with a d -spacing ratio of 1, $(1/3)^{1/2}$, and $(1/4)^{1/2}$, corresponding to Miller indices; 10, 11, and 20, respectively. For example, a diffraction pattern with a d -spacing at 31.90 Å, 18.44 Å, 16.03 Å and a broad diffuse peak (4.59 Å) at wide-angle region was observed for compound **2a** ($n=14$) and this diffraction pattern corresponded to a hexagonal columnar arrangement (see Fig. 9). This pattern corresponds to an intercolumnar distance or lattice constant (i.e., a parameter of the hexagonal lattice) of 36.7 Å. All compounds **1a** gave similar diffraction patterns as compounds **2a**. Interestingly, the lattice constants of

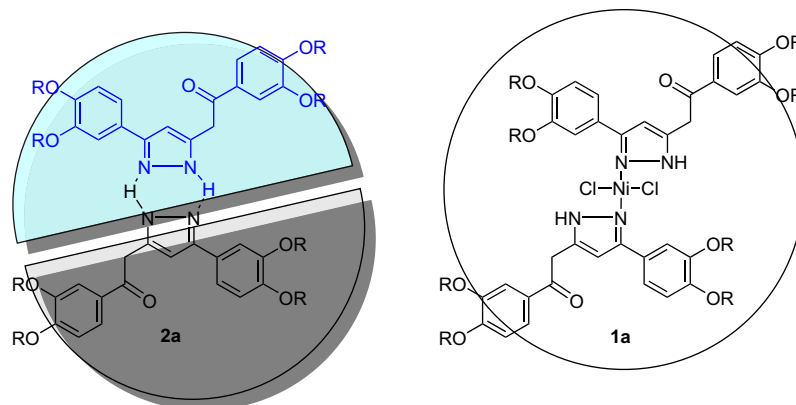


Figure 7. Schematic representation of proposed structures for the formation of columnar phases in compounds **2a** and **1a**. The dashed line in **2a** is an intermolecular H-bonding.

Table 5
Variable-temperature XRD diffraction data for compounds **1a**, **2a,2b**, and **4**

Compound	Mesophase/ $^{\circ}$ C	Lattice constant/ \AA	<i>d</i> -Spacing/ \AA obsd	Miller indices
2b (<i>n</i> =6)	SmA (130 $^{\circ}$ C)	—	28.70 (30.08 ^a)	001
2b (<i>n</i> =10)	SmC (145 $^{\circ}$ C)	—	33.04 (41.06 ^a)	001
2b (<i>n</i> =12)	SmC (150 $^{\circ}$ C)	—	37.21 (47.43 ^a)	001
4 (<i>n</i> =6)	SmA (109 $^{\circ}$ C)	—	24.47 (30.08 ^a)	001
	SmC (96 $^{\circ}$ C)	—	24.08 (30.08 ^a)	001
2a (<i>n</i> =12)	Col _h (80 $^{\circ}$ C)	<i>a</i> =34.32	29.72 (29.72)	100
			4.56	halo
2a (<i>n</i> =14)	Col _h (80 $^{\circ}$ C)	<i>a</i> =36.70	31.90 (31.90)	10
			18.44 (18.42)	11
			16.03 (15.95)	20
			4.59	halo
1a (<i>n</i> =12)	Col _h (104 $^{\circ}$ C)	<i>a</i> =33.82	29.29 (29.29)	10
			16.93 (16.91)	11
			4.61	halo
1a (<i>n</i> =14)	Col _h (120 $^{\circ}$ C)	<i>a</i> =35.76	30.97 (30.97)	10
			17.89 (17.88)	11
			15.57 (15.48)	20
			4.60	halo
1a (<i>n</i> =16)	Col _h (115 $^{\circ}$ C)	<i>a</i> =37.44	32.42 (32.42)	10
			18.70 (18.72)	11
			16.23 (16.21)	20
			4.64	halo

^a Molecular length estimated by MM2 model.

two compounds **2a** and **1a** were quite similar in value, indicating that the size or the diameter of the columns formed in hexagonal columnar phases was approximately equal.

3. Conclusions

A new series of unsymmetrical pyrazoles **2a,2b** and their nickel(II) complexes **1a** were prepared and mesomorphic properties investigated. All compounds formed mesomorphic behavior. Nickel ion preferred the square-planar coordination, which favored the molecular packings. A dimeric structure formed by intermolecular H-bonding was used to induce the formation of the mesophases in such system. Other metal complexes might be prepared in future.

4. Experimental

4.1. General

All chemicals and solvents were reagent grade from Aldrich Chemical Co., and all solvents were dried by standard techniques. ¹H and ¹³C NMR spectra were measured on a Bruker DRS-200. DSC

thermographs were carried out on a Mettler DSC 822 and calibrated with a pure indium sample. All phase transitions are determined by a scan rate of 10.0 $^{\circ}$ /min. Optical polarized microscopy was carried out on Zeiss Axioplan 2 equipped with a hot stage system of Mettler FP90/FP82HT. Elemental analyses were performed on a Heraeus CHN-O-Rapid elemental analyzer. The powder diffraction data were collected from the Wiggler-A beamline of the National Synchrotron Radiation Research Center (NSRRC) with the wavelength of 1.3263 \AA . Diffraction patterns were recorded in $\theta/2\theta$ geometry with step scans normally 0.02 $^{\circ}$ in $2\theta=1-10^{\circ}$ step $^{-1}$ s $^{-1}$ and 0.05 $^{\circ}$ in $2\theta=10-25^{\circ}$ step $^{-1}$ s $^{-1}$ and a gas flow heater was used to control the temperature. The powder samples were charged in Lindemann capillary tubes (80 mm long and 0.01 mm thick) from Charles Supper Co. with an inner diameter of 1.0 mm.

4.2. 1,5-Bis(3,4-bis(dodecyloxy)phenyl)pentane-1,3,5-trione (**3a**; *n*=12)

Yellow powder, yield 60%. ¹H NMR (CDCl₃): δ 0.85 (t, *J*=6.45 Hz, -CH₃, 12H), 1.23–1.84 (m, -CH₂, 80H), 4.02 (t, *J*=4.2 Hz, -CH₂, 8H),

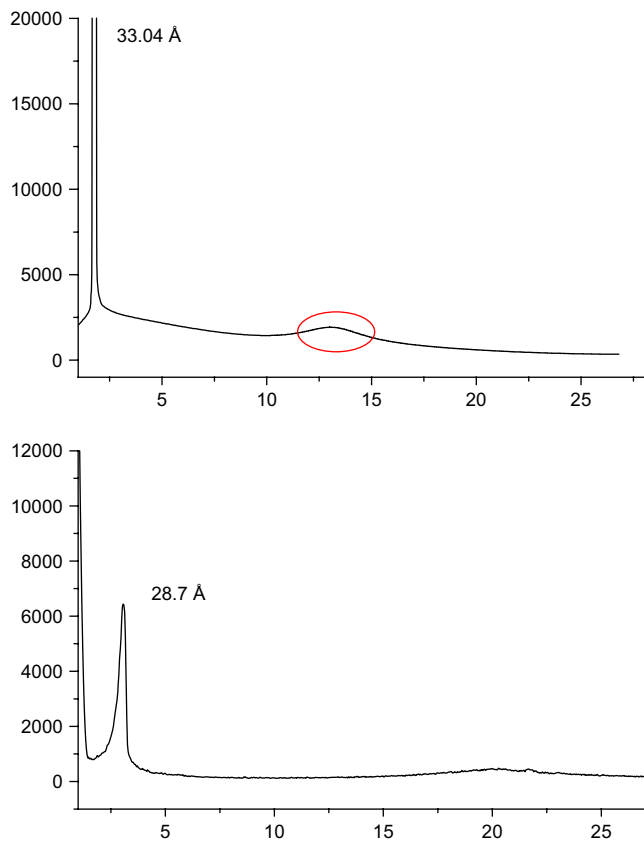


Figure 8. The powder X-ray diffraction patterns for compounds; **2b** ($n=10$, top plot) at 145.0 °C and **2b** ($n=6$, bottom plot) at 130.0 °C.

[5.88 (s), 6.20 (s)] (OCCHCO, 2H), [6.84 (d), 7.40 (d), 7.53 (d), 7.60 (d)] (*ArH*, 6H), [14.84 (s), 16.06 (s)] (COH, 2H). ^{13}C NMR (CDCl_3): δ 14.09, 22.69, 26.01, 29.02, 29.09, 29.14, 29.24, 29.38, 29.64, 31.93, 50.14, 69.05, 69.23, 69.39, 95.51, 96.19, 111.61, 112.05, 112.16, 112.58, 112.79, 120.21, 121.44, 123.99, 126.25, 126.69, 129.29, 148.94, 149.00, 152.42, 153.35, 154.14, 173.43, 183.21, 188.64, 192.50, 193.00.

4.3. 1,5-Bis(4-(dodecyloxy)phenyl)pentane-1,3,5-trione (**3b**; $n=12$)

Yellow powder, yield 68%. ^1H NMR (CDCl_3): δ 0.84 (t, $J=6.6$ Hz, $-\text{CH}_3$, 6H), 1.23–1.78 (m, $-\text{CH}_2$, 40H), 3.98 (t, $J=3.3$ Hz, $-\text{CH}_2$, 4H), [5.88 (s), 6.20 (s)] (OCCHCO, 2H), [$J=1.5$ Hz, 6.91 (d), $J=0.9$ Hz, 7.77 (d), $J=9$ Hz, 7.96 (d)] (*ArH*, 8H), [14.84 (s), 16.06 (s)] (COH, 2H). ^{13}C NMR (CDCl_3): δ 13.98, 22.56, 25.85, 28.98, 29.03, 29.23, 29.46, 29.52, 31.80, 50.21, 53.24, 68.14, 68.22, 95.19, 95.90, 114.05, 114.31, 125.77, 126.18, 128.04, 128.92, 129.10, 130.90, 131.16, 132.15, 161.99, 162.85, 163.57, 170.48, 173.20, 182.50, 184.46, 189.19, 192.32, 192.62, 193.11.

4.4. 1-(3,4-Bis(dodecyloxy)phenyl)-2-(3-(3,4-bis(dodecyloxy)phenyl)-1H-pyrazol-5-yl)ethanone (**2a**; $n=12$)

White powder, yield 78%. ^1H NMR (CDCl_3): δ 0.84 (t, $J=6.45$ Hz, $-\text{CH}_3$, 12H), 1.22–1.78 (m, $-\text{CH}_2$, 80H), 3.98 (t, $J=6.3$ Hz, $-\text{CH}_2$, 8H), 4.57 (s, $\text{COCH}_2\text{C}=\text{C}$, 2H), 6.61 (s, $=\text{CH}-\text{C}=\text{N}$, 1H), [6.85 (d), 7.38 (d), 7.51 (d), 7.67 (d)] (*ArH*, 6H). ^{13}C NMR (CDCl_3): δ 14.09, 22.69, 26.05, 29.07, 29.18, 29.38, 29.48, 29.67, 31.93, 36.32, 69.03, 69.24, 69.35, 102.61, 111.55, 112.51, 113.73, 118.74, 123.08, 123.55, 128.87, 142.66, 147.87, 148.98, 149.42, 149.72,

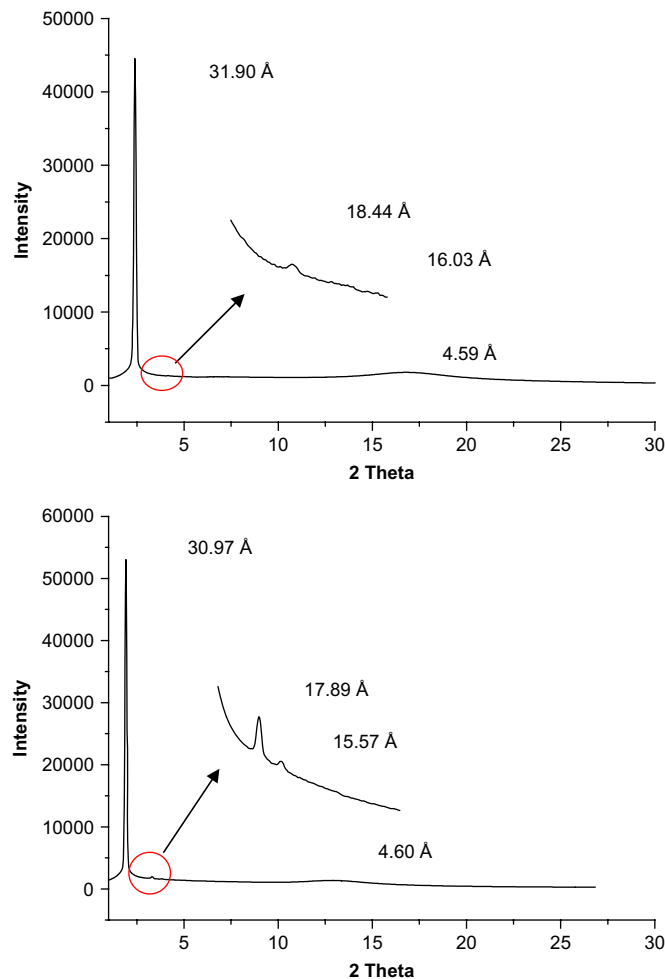


Figure 9. The powder X-ray diffraction patterns for compounds; **2a** ($n=14$, top plot) at 80.0 °C and **1a** ($n=6$, bottom plot) at 120.0 °C.

154.02, 194.24. Anal. Calcd for $\text{C}_{65}\text{H}_{110}\text{N}_2\text{O}_5$: C, 78.10; H, 11.09. Found: C, 77.90; H, 11.04.

4.5. 1-(3,4-Bis(hexyloxy)phenyl)-2-(3-(3,4-bis(hexyloxy)phenyl)-1H-pyrazol-5-yl)ethanone (**2a**; $n=6$)

White powder, yield 68%. ^1H NMR (CDCl_3): δ 0.92 (t, $J=2.4$ Hz, $-\text{CH}_3$, 12H), 1.35–1.85 (m, $-\text{CH}_2$, 32H), 4.00 (t, $J=3.15$ Hz, $-\text{CH}_2$, 8H), 4.34 (s, $-\text{CH}_2\text{C}$, 2H), 6.45 (s, $-\text{CH}-\text{CN}$, 1H), [6.85 (d), 7.29 (d), 7.54 (d), 7.59 (d)] (*ArH*, 6H). ^{13}C NMR (CDCl_3): δ 13.91, 22.50, 25.60, 28.90, 29.00, 29.16, 31.47, 31.51, 36.46, 68.92, 69.10, 69.17, 102.26, 111.26, 111.43, 112.44, 113.65, 118.36, 123.48, 123.83, 128.86, 142.53, 147.94, 148.86, 149.27, 153.86, 194.68. Anal. Calcd for $\text{C}_{41}\text{H}_{62}\text{N}_2\text{O}_5$: C, 74.28; H, 9.43. Found: C, 74.56; H, 9.56.

4.6. 1-(3,4-Bis(octyloxy)phenyl)-2-(3-(3,4-bis(octyloxy)phenyl)-1H-pyrazol-5-yl)ethanone (**2a**; $n=8$)

White powder, yield 70%. ^1H NMR (CDCl_3): δ 0.84 (t, $J=6.3$ Hz, $-\text{CH}_3$, 12H), 1.24–1.79 (m, $-\text{CH}_2$, 48H), 3.96 (t, $J=5.25$ Hz, $-\text{CH}_2$, 8H), 4.29 (s, $-\text{CH}_2\text{C}$, 2H), 6.39 (s, $-\text{CH}-\text{CN}$, 1H), [6.79 (d), 7.17 (d), 7.49 (d), 7.56 (d)] (*ArH*, 6H). ^{13}C NMR (CDCl_3): δ 13.97, 22.57, 25.94, 28.96, 29.07, 29.18, 31.73, 36.13, 68.94, 69.16, 69.28, 102.70, 111.30, 111.49, 112.45, 113.62, 118.76, 123.45, 128.78, 142.54, 147.80, 148.90, 149.27, 153.95, 194.00. Anal. Calcd for $\text{C}_{49}\text{H}_{78}\text{N}_2\text{O}_5$: C, 75.92; H, 10.14. Found: C, 76.12; H, 10.11.

4.7. 1-(3,4-Bis(decyloxy)phenyl)-2-(3-(3,4-bis(decyloxy)phenyl)-1H-pyrazol-5-yl)ethanone (2a; n = 10)

White powder, yield 75%. ¹H NMR (CDCl₃): δ 0.85 (t, J=6.0 Hz, -CH₃, 12H), 1.24–1.80 (m, -CH₂, 64H), 3.98 (t, J=5.4 Hz, -CH₂, 8H), 4.33 (s, -CH₂C, 2H), 6.45 (s, -CH-CN, 1H), [6.81 (d), 7.30 (d), 7.49 (d), 7.56 (d)] (ArH, 6H). ¹³C NMR (CDCl₃): δ 14.08, 22.68, 26.04, 29.06, 29.17, 29.36, 29.46, 29.61, 31.92, 36.27, 69.02, 69.23, 69.34, 102.70, 111.55, 112.51, 113.70, 118.78, 123.55, 128.87, 142.65, 147.87, 148.39, 148.97, 149.42, 154.01, 194.17. Anal. Calcd for C₅₇H₉₄N₂O₅: C, 77.15; H, 10.68. Found: C, 77.42; H, 10.68.

4.8. 1-(3,4-Bis(tetradecyloxy)phenyl)-2-(3-(3,4-bis(tetradecyloxy)phenyl)-1H-pyrazol-5-yl)ethanone (2a; n = 14)

White powder, yield 72%. ¹H NMR (CDCl₃): δ 0.84 (t, J=6.0 Hz, -CH₃, 12H), 1.22–1.78 (m, -CH₂, 96H), 3.98 (t, J=6.75 Hz, -CH₂, 8H), 4.46 (s, -CH₂C, 2H), 6.58 (s, -CH-CN, 1H), [6.82 (d), 7.34 (d), 7.46 (d), 7.59 (d)] (ArH, 6H). ¹³C NMR (CDCl₃): δ 14.09, 22.68, 26.05, 29.06, 29.17, 29.37, 29.68, 29.72, 31.93, 36.23, 69.05, 69.25, 69.39, 111.58, 112.53, 113.72, 118.81, 122.91, 123.52, 128.86, 149.00, 149.44, 149.83, 154.06, 194.11. Anal. Calcd for C₇₃H₁₂₆N₂O₅: C, 78.86; H, 11.42. Found: C, 78.93; H, 11.43.

4.9. 1-(3,4-Bis(hexadecyloxy)phenyl)-2-(3-(3,4-bis(hexadecyloxy)phenyl)-1H-pyrazol-5-yl)ethanone (2a; n = 16)

White powder, yield 68%. ¹H NMR (CDCl₃): δ 0.84 (t, J=6.45 Hz, -CH₃, 12H), 1.23–1.82 (m, -CH₂, 112H), 4.03 (t, J=8.7 Hz, -CH₂, 8H), 4.57 (s, -CH₂C, 2H), 6.61 (s, -CH-CN, 1H), [6.87 (d), 7.47 (d), 7.51 (d), 7.67 (d)] (ArH, 6H). Anal. Calcd for C₈₁H₁₄₂N₂O₅: C, 79.48; H, 11.69. Found: C, 79.45; H, 11.70.

4.10. 1-(4-Dodecyloxyphenyl)-2-(3-(4-dodecyloxyphenyl)-1H-pyrazol-5-yl)ethanone (2b; n = 12)

To a solution of 1,5-bis(4-(dodecyloxy)phenyl)pentane-1,3,5-trione (5.0 g, 7.87 mmol) dissolved in absolute ethanol (45 mL) was added hydrazine monohydrate (0.43 g, 8.66 mmol), and the mixture was refluxed for 2 h under nitrogen atmosphere. The ethanol was removed under vacuum. The off-white residue was then purified by recrystallization from THF/MeOH. The product was isolated as white powder with a yield of 75%. ¹H NMR (CDCl₃): δ 0.85 (t, J=6.75 Hz, -CH₃, 6H), 1.23–1.80 (m, -CH₂, 40H), 3.97 (t, J=4.2 Hz, -OCH₂, 4H), 4.32 (s, -CH₂C, 2H), 6.39 (s, -CH-CN, 1H), [J=1.5 Hz, 6.89 (d), J=8.4 Hz, 7.54 (d), J=8.4 Hz, 7.97 (d)] (ArH, 8H). Anal. Calcd for C₄₁H₆₂N₂O₃: C, 78.05; H, 9.90. Found: C, 77.74; H, 9.86.

4.11. 1-(4-Hexyloxyphenyl)-2-(3-(4-hexyloxyphenyl)-1H-pyrazol-5-yl)ethanone (2b; n = 6)

White powder, yield 70%. ¹H NMR (CDCl₃): δ 0.85 (t, -CH₃, 6H), 1.32–1.78 (m, -CH₂, 16H), 3.94 (t, J=4.05 Hz, -OCH₂, 4H), 4.30 (s, -CH₂C, 2H), 6.37 (s, -CH-CN, 1H), [J=3.60 Hz, 6.87 (d), J=6.90 Hz, 7.54 (d), J=1.80 Hz, 7.98 (d)] (ArH, 8H). ¹³C NMR (CDCl₃): δ 13.98, 22.56, 25.61, 25.67, 29.01, 29.17, 31.05, 31.56, 36.44, 68.06, 68.30, 102.59, 114.03, 114.33, 122.65, 127.22, 128.81, 130.92, 142.57, 147.63, 159.58, 163.52, 194.15. Anal. Calcd for C₂₉H₃₈N₂O₃: C, 75.29; H, 8.28. Found: C, 75.13; H, 8.43.

4.12. 1-(4-Octyloxyphenyl)-2-(3-(4-octyloxyphenyl)-1H-pyrazol-5-yl)ethanone (2b; n = 8)

White powder, yield 71%. ¹H NMR (CDCl₃): δ 0.85 (t, J=6.45 Hz, -CH₃, 6H), 1.25–1.78 (m, -CH₂, 24H), 3.92 (t, J=7.35 Hz, -CH₂, 4H),

4.30 (s, -CH₂C, 2H), 6.37 (s, -CH-CN, 1H), [J=3.0 Hz, 6.88 (d), J=8.40 Hz, 7.52 (d), J=9.00 Hz, 7.96 (d)] (ArH, 8H). ¹³C NMR (CDCl₃): δ 13.05, 21.60, 24.92, 24.99, 28.20, 28.26, 28.32, 30.76, 35.66, 67.04, 67.29, 101.22, 113.3, 113.75, 122.43, 125.93, 127.86, 129.92, 141.62, 146.80, 158.27, 162.48, 193.66. Anal. Calcd for C₃₃H₄₆N₂O₃: C, 76.41; H, 8.94. Found: C, 76.11; H, 9.03.

4.13. 1-(4-Decyloxyphenyl)-2-(3-(4-decyloxyphenyl)-1H-pyrazol-5-yl)ethanone (2b; n = 10)

White powder, yield 71%. ¹H NMR (CDCl₃): δ 0.85 (t, J=6.0 Hz, -CH₃, 6H), 1.40–2.14 (m, -CH₂, 32H), 3.94 (t, J=7.35 Hz, -CH₂, 4H), 4.32 (s, -CH₂C, 2H), 6.38 (s, -CH-CN, 1H), [J=1.8 Hz, 6.89 (d), J=8.4 Hz, 7.53 (d), J=8.1 Hz, 7.97 (d)] (ArH, 8H). ¹³C NMR (CDCl₃): δ 13.91, 22.48, 25.85, 29.37, 31.71, 68.16, 102.30, 114.20, 114.66, 126.72, 126.97, 130.77, 131.97, 147.64, 159.35, 194.20. Anal. Calcd for C₃₇H₅₄N₂O₃: C, 77.31; H, 9.47. Found: C, 77.30; H, 9.58.

4.14. 1-(4-Tetradecyloxyphenyl)-2-(3-(4-tetradecyloxyphenyl)-1H-pyrazol-5-yl)ethanone (2b; n = 14)

White powder, yield 72%. ¹H NMR (CDCl₃): δ 0.85 (t, J=6.6 Hz, -CH₃, 6H), 1.23–1.69 (m, -CH₂, 48H), 3.97 (t, J=6.9 Hz, -CH₂, 4H), 4.32 (s, -CH₂C, 2H), 6.38 (s, -CH-CN, 1H), [J=7.2 Hz, 6.90 (d), J=7.5 Hz, 7.52 (d), J=9.3 Hz, 7.98 (d)] (ArH, 8H). Anal. Calcd for C₄₅H₇₀N₂O₃: C, 78.67; H, 10.27. Found: C, 78.38; H, 10.26.

4.15. 1-(4-Hexadecyloxyphenyl)-2-(3-(4-hexadecyloxyphenyl)-1H-pyrazol-5-yl)ethanone (2b; n = 16)

White powder, yield 75%. ¹H NMR (CDCl₃): δ 0.84 (t, -CH₃, 6H), 1.22–1.82 (m, -CH₂, 56H), 3.96 (t, J=7.05 Hz, -CH₂, 4H), 4.32 (s, -CH₂C, 2H), 6.38 (s, -CH-CN, 1H), [J=7.2 Hz, 6.90 (d), J=6.9 Hz, 7.53 (d), J=7.8 Hz, 7.97 (d)] (ArH, 8H). Anal. Calcd for C₄₉H₇₈N₂O₃: C, 79.19; H, 10.58. Found: C, 78.91; H, 10.59.

4.16. Nickel complexes of 1-(3,4-bis(dodecyloxy)phenyl)-2-(3-(3,4-bis(dodecyloxy)phenyl)-1H-pyrazol-5-yl)ethanone (1a; n = 12)

To a solution of 1-(3,4-bis(dodecyloxy)phenyl)-2-(3-(3,4-bis(dodecyloxy)phenyl)-1H-pyrazol-5-yl)ethanone (0.400 g, 0.400 mmol) dissolved in 20 mL ethanol was added nickel(II) chloride. The solution was refluxed for 24 h. The solution was concentrated to dryness, and the residue was purified by recrystallization from THF/CH₃OH. The product was isolated as light green solids. Yield 70%. Anal. Calcd for C₁₃₀H₂₂₀N₄O₁₀NiCl₂: C, 73.35; H, 10.42; N, 2.63. Found: C, 73.99; H, 10.75; N, 2.61. Compound **1a** (n=14). Anal. Calcd for C₁₄₆H₂₅₂N₄O₁₀NiCl₂: C, 74.52; H, 10.79; N, 2.38. Found: C, 74.59; H, 10.95; N, 2.38. Compound **1a** (n=16). Anal. Calcd for C₁₆₂H₂₈₄N₄O₁₀NiCl₂: C, 75.49; H, 11.11. Found: C, 75.34; H, 11.02.

4.17. 1-(4-(Dodecyloxy)phenyl)-2-(3-(4-(dodecyloxy)phenyl)-isoxazol-5-yl)ethanone (4; n = 12)

To a solution of 1,5-bis(4-(dodecyloxy)phenyl)pentane-1,3,5-trione (5.0 g, 7.87 mmol) dissolved in 35 mL of absolute ethanol was added hydroxylamine hydrochloride (0.6 g, 8.66 mmol) under nitrogen atmosphere. The solution was gently refluxed for 2 h. The solution was then stirred at room temperature for 12 h. The solvent was removed under reduced pressure, and the product isolated as white powder was obtained after recrystallization from THF/MeOH. Yield 75%. ¹H NMR (CDCl₃): δ 0.85 (t, J=6.75 Hz, -CH₃, 6H), 1.24–1.77 (m, -CH₂, 40H), 3.98 (t, J=4.5 Hz, -CH₂, 4H), [4.31, 4.40] (s, -CH₂C, 2H), [6.41, 6.50] (s, -CH-CN, 1H), [J=8.7 Hz, 6.92 (d),

$J=1.2$ Hz, 7.67 (d), $J=2.4$ Hz, 7.99 (d)] (*ArH*, 8H). ^{13}C NMR (CDCl_3): δ 14.10, 22.68, 25.96, 29.06, 29.16, 29.34, 29.57, 29.63, 31.91, 36.15, 36.60, 68.17, 68.36, 98.82, 101.35, 114.42, 114.51, 114.83, 120.05, 121.34, 127.38, 128.16, 128.83, 131.00, 160.68, 163.65, 166.36, 170.22, 193.35. Anal. Calcd for $\text{C}_{41}\text{H}_{61}\text{NO}_4$: C, 77.93; H, 9.73. Found: C, 78.14; H, 9.76.

4.18. 1-(4-(Hexyloxy)phenyl)-2-(3-(4-(hexyloxy)phenyl)-isoxazol-5-yl)ethanone (4; $n=6$)

White powder, yield 61%. ^1H NMR (CDCl_3): δ 0.88 (t, $-\text{CH}_3$, 6H), 1.31–1.76 (m, $-\text{CH}_2$, 16H), 3.98 (t, $J=7.8$ Hz, $-\text{CH}_2$, 4H), [4.30, 4.38] (s, $-\text{CH}_2\text{C}$, 2H), [6.41, 6.50] (s, $-\text{CH}-\text{CN}$, 1H), [$J=8.7$ Hz, 6.92 (d), $J=9$ Hz, 7.66 (d), $J=9$ Hz, 7.98 (d)] (*ArH*, 8H). ^{13}C NMR (CDCl_3): δ 13.94, 22.51, 25.57, 25.62, 28.96, 29.07, 31.46, 31.50, 36.10, 68.12, 98.74, 101.29, 114.36, 114.46, 114.78, 120.00, 127.33, 128.77, 130.96, 158.84, 160.62, 163.59, 170.15, 193.31. Anal. Calcd for $\text{C}_{29}\text{H}_{37}\text{NO}_4$: C, 75.13; H, 8.04. Found: C, 75.34; H, 8.06.

4.19. 1-(4-(Heptyloxy)phenyl)-2-(3-(4-(heptyloxy)phenyl)-isoxazol-5-yl)ethanone (4; $n=7$)

White powder, yield 62%. ^1H NMR (CDCl_3): δ 0.86 (t, $-\text{CH}_3$, 6H), 1.28–1.57 (m, $-\text{CH}_2$, 20H), 3.99 (t, $J=7.8$ Hz, $-\text{CH}_2$, 4H), [4.30, 4.39] (s, $-\text{CH}_2\text{C}$, 2H), [6.41, 6.50] (s, $-\text{CH}-\text{CN}$, 1H), [$J=8.7$ Hz, 6.92 (d), $J=8.7$ Hz, 7.66 (d), $J=9.0$ Hz, 7.98 (d)] (*ArH*, 8H). ^{13}C NMR (CDCl_3): δ 13.95, 22.48, 25.81, 28.93, 29.06, 31.07, 31.64, 34.06, 36.05, 36.49, 68.07, 68.25, 98.70, 101.24, 114.31, 114.41, 114.73, 119.95, 127.28, 128.06, 128.72, 130.90, 158.79, 162.24, 163.54, 170.10, 193.25. Anal. Calcd for $\text{C}_{31}\text{H}_{41}\text{NO}_4$: C, 75.73; H, 8.41. Found: C, 75.84; H, 8.46.

4.20. 1-(4-(Octyloxy)phenyl)-2-(3-(4-(octyloxy)phenyl)-isoxazol-5-yl)ethanone (4; $n=8$)

White powder, yield 60%. ^1H NMR (CDCl_3): δ 0.86 (t, $-\text{CH}_3$, 6H), 1.26–1.78 (m, $-\text{CH}_2$, 24H), 3.96 (t, $J=3.3$ Hz, $-\text{CH}_2$, 4H), [4.30, 4.38] (s, $-\text{CH}_2\text{C}$, 2H), [6.41, 6.50] (s, $-\text{CH}-\text{CN}$, 1H), [$J=9.0$ Hz, 6.92 (d), $J=8.7$ Hz, 7.65 (d), $J=6.3$ Hz, 7.98 (d)] (*ArH*, 8H). ^{13}C NMR (CDCl_3): δ 13.94, 22.50, 25.82, 25.86, 28.93, 29.07, 29.16, 31.65, 36.00, 68.03, 68.22, 98.70, 101.22, 114.28, 114.37, 114.70, 119.92, 127.24, 128.02, 128.70, 130.86, 158.77, 160.54, 163.50, 170.06, 193.19. Anal. Calcd for $\text{C}_{33}\text{H}_{45}\text{NO}_4$: C, 76.26; H, 8.73. Found: C, 76.11; H, 8.85.

Acknowledgements

We thank the National Science Council of Taiwan, ROC (NSC 96-2113-M-008-MY2 and NSC 96-2752-M-008-010-PAE) in generous support of this work.

References and notes

- (a) *Structure and Bonding*; Donnio, B., Bruce, D. W., Eds.; Springer: Berlin, Heidelberg, 1999; Vol. 95, pp 194–217; (b) Hudson, S. A.; Maitlis, P. M. *Chem. Rev.* **1993**, *93*, 861–885; (c) Espinet, P.; Esteruelas, M. A.; Oro, L. A.; Serrano, J. L.; Sola, E. *Coord. Chem. Rev.* **1992**, *117*, 215–274; (d) *Metallomesogens; Synthesis, Properties, and Applications*; Serrano, J. L., Ed.; VCH: New York, NY, 1996; (e)

- Giroud-Godquin, A. M.; Maitlis, P. M. *Angew. Chem., Int. Ed. Engl.* **1991**, *30*, 375–402; (f) Giroud-Godquin, A. M. *Coord. Chem. Rev.* **1998**, *178*, 1485–1499.
- (a) Sereidyuk, M.; Gaspar, A. B.; Ksenofontov, V.; Galyametdinov, Y.; Kusz, J.; Guütlich, P. *J. Am. Chem. Soc.* **2008**, *130*, 1431–1439; (b) Zheng, H.; Swager, T. M. *J. Am. Chem. Soc.* **1994**, *116*, 761–762; (c) Trzaska, S. T.; Hsu, H. F.; Swager, T. M. *J. Am. Chem. Soc.* **1999**, *121*, 4518–4519; (d) Cardinaels, T.; Ramaekers, J.; Guillon, D.; Donnio, B.; Binnemans, K. *J. Am. Chem. Soc.* **2005**, *127*, 17602–17603.
- Trofimenko, S. *Chem. Rev.* **1972**, *72*, 497–509.
- (a) Trofimenko, S. *Prog. Inorg. Chem.* **1986**, *34*, 115–210; (b) Niedenzu, K.; Trofimenko, S. *Top. Curr. Chem.* **1986**, *131*, 1–37.
- (a) La Monica, G.; Ardizzoia, G. A. *Prog. Inorg. Chem.* **1997**, *46*, 151–238; (b) Eigenbrot, C. W., Jr.; Raymond, K. N. *Inorg. Chem.* **1982**, *21*, 2653–2660; (c) Röttger, D.; Erker, G.; Grehl, M.; Frölich, R. *Organometallics* **1994**, *13*, 3897–3902.
- (a) Rasika Dias, H. V.; Palehepitiya Gamage, C. S.; Keltner, J.; Diyabalanage, H. V. K.; Omara, I.; Eyobo, Y.; Dias, N. R.; Roehr, N.; McKinney, L.; Poth, T. *Inorg. Chem.* **2007**, *46*, 2979–2987; (b) Mohamed, A. A.; Pérez, L. M.; Fackler, J. P. *Inorg. Chim. Acta* **2005**, *358*, 1657–1662; (c) Kishimura, A.; Yamashita, T.; Aida, T. *J. Am. Chem. Soc.* **2005**, *127*, 179–183; (d) Dias, H. V. R.; Diyabalanage, H. V. K.; Eldabaja, M. G.; Elbjeirami, O.; Rawashdeh-Omary, M. A.; Omary, M. A. *J. Am. Chem. Soc.* **2005**, *127*, 7489–7501; (e) Dias, H. V. R.; Diyabalanage, H. V. K. *Polyhedron* **2006**, *25*, 1655–1661; (f) Grimes, T.; Omary, M. A.; Dias, H. V. R.; Cundari, T. R. *J. Phys. Chem. A* **2006**, *110*, 5823–5830; (g) Dias, H. V. R.; Diyabalanage, H. V. K.; Gamage, C. S. *P. Chem. Commun.* **2005**, 1619–1621.
- (a) Wang, Z.; Abernethy, C. D.; Cowley, A. H.; Jones, J. N.; Jones, R. A.; Macdonald, C. L. B.; Zhang, L. *J. Organomet. Chem.* **2003**, *666*, 35–42; (b) Guzei, I. A.; Baboul, A. G.; Yap, G. P. A.; Rheigold, A. L.; Schlegel, B.; Winter, C. H. *J. Am. Chem. Soc.* **1997**, *119*, 3387–3388.
- (a) Ehlert, M. K.; Rettig, S. J.; Storr, A.; Thompson, R. C.; Trotter, J. *Can. J. Chem.* **1990**, *68*, 1444–1449; (b) Ardizzoia, G. A.; Cenine, S.; Monica, G. L.; Masciocchi, N.; Maspero, A.; Moret, M. *Inorg. Chem.* **1998**, *37*, 4284–4292.
- (a) Ardizzoia, G. A.; Cenine, S.; Monica, G. L.; Masciocchi, N.; Moret, M. *Inorg. Chem.* **1994**, *33*, 1458–1463; (b) Kavlakoglu, E.; Elmali, A.; Elerman, Y.; Svoboda, I. *Polyhedron* **2002**, *21*, 1539–1545.
- (a) Torralba, M. C.; Cano, M.; Campo, J. A.; Heras, J. V.; Pinilla, E.; Torres, M. R. *J. Organomet. Chem.* **2006**, *691*, 765–778; (b) Torralba, M. C.; Campo, J. A.; Heras, J. V.; Bruce, D. W.; Cano, M. *Dalton Trans.* **2006**, 3918–3926; (c) Barberá, J.; Elduque, A.; Giménez, R.; Lahoz, F. L.; López, J. A.; Oro, L. A.; Serrano, J. L.; Villacampa, B.; Villalba, J. *Inorg. Chem.* **1999**, *38*, 3085–3092.
- Barberá, J.; Cativiela, C.; Serrano, J. L.; Zurbano, M. M. *Liq. Cryst.* **1992**, *11*, 887–897.
- Diez-Barra, E.; Hoz, A. d. l.; Sánchez-Migallón, A.; Tejada, J. *Heterocycles* **1992**, *34*, 1365–1373.
- Giménez, R.; Manrique, A. B.; Uriel, S.; Barberá, J.; Serrano, J. L. *Chem. Commun.* **2004**, 2064–2065.
- (a) Bouwman, E.; Driessen, W. L.; Graaff, R. A. G.; deReedijk, J. *Acta Crystallogr., Sect. C* **1984**, *40*, 1562–1563; (b) Bovio, B.; Cingolani, A.; Bonati, F. *Z. Anorg. Allg. Chem.* **1992**, *610*, 151–156.
- (a) Torralba, M. C.; Cano, M.; Campo, J. A.; Heras, J. V.; Pinilla, E.; Torres, M. R. *J. Organomet. Chem.* **2001**, *633*, 91–104; (b) Torralba, M. C.; Cano, M.; Campo, J. A.; Heras, J. V.; Pinilla, E.; Torres, M. R. *J. Organomet. Chem.* **2002**, *654*, 150–161.
- (a) Canom, N.; Heras, J. V.; Maeso, M.; Alvaro, M.; Fernfindez, R.; Pinilla, E.; Campo, J. A.; Monge, A. *J. Organomet. Chem.* **1997**, *534*, 159–172; (b) López, C.; Jiménez, J. A.; Claramunt, R. M.; Cano, M.; Heras, J. V.; Campo, J. A.; Pinilla, E.; Monge, A. *J. Organomet. Chem.* **1996**, *511*, 115–127.
- (a) Torralba, M. C.; Cano, M.; Campo, J. A.; Heras, J. V.; Pinilla, E. *Z. New Cryst. Struct.* **2005**, *220*, 615–616; (b) Torralba, M. C.; Cano, M.; Campo, J. A.; Heras, J. V.; Pinilla, E.; Torres, M. R. *Inorg. Chem. Commun.* **2002**, *5*, 887–890; (c) Mayoral, M. J.; Torralba, M. C.; Cano, M.; Campo, J. A.; Heras, J. V. *Inorg. Chem. Commun.* **2003**, *6*, 626–629; (d) Torralba, M. C.; Cano, M.; Gómez, S.; Campo, J. A.; Heras, J. V.; Perles, J.; Ruiz-Valero, C. *J. Organomet. Chem.* **2003**, *682*, 26–34; (e) Torralba, M. C.; Cano, M.; Campo, J. A.; Heras, J. V.; Pinilla, E.; Torres, M. R. *Inorg. Chem. Commun.* **2006**, *9*, 1271–1275.
- Henslee, G. H.; Oliver, J. D. *J. Cryst. Mol. Struct.* **1977**, *7*, 137–146.
- (a) Lin, H. D.; Lai, C. K. *J. Chem. Soc., Dalton Trans.* **2001**, 2383–2387; (b) Barberá, J.; Elduque, A.; Giménez, R.; Oro, L. A.; Serrano, J. L. *Angew. Chem., Int. Ed.* **1996**, *35*, 2832–2835; (c) Barberá, J.; Giménez, R.; Serrano, J. L. *Chem. Mater.* **2000**, *12*, 481–489; (d) Barberá, J.; Elduque, A.; Giménez, R.; Lahoz, F.; López, J. A.; Oro, L. A.; Serrano, J. L. *Inorg. Chem.* **1998**, *37*, 2960–2967; (e) Kim, S. J.; Kang, S. H.; Park, K. M.; Kim, H.; Zin, W. C.; Choi, M. G.; Kim, K. *Chem. Mater.* **1998**, *10*, 1889–1893; (f) Giménez, R.; Elduque, A.; López, J. A.; Barberá, J.; Cavero, E.; Lantero, I.; Oro, L. A.; Serrano, J. L. *Inorg. Chem.* **2006**, *45*, 10363–10370.
- (a) Shen, W. C.; Wang, Y. J.; Cheng, K. L.; Lee, G. H.; Lai, C. K. *Tetrahedron* **2006**, *62*, 8035–8044; (b) Cativiela, C.; Serrano, J. L.; Zurbano, M. M. *J. Org. Chem.* **1995**, *60*, 3074–3083.